

Multicolored quantum dimer models, resonating valence–bond states, color visons, and the triangular–lattice t_{2g} spin–orbital system

B. Normand¹

¹*Department of Physics, Renmin University of China, Zhongguancun Ave. 59, Beijing 100872, China*
(Dated: October 17, 2018)

The spin–orbital model for triply degenerate t_{2g} electrons on a triangular lattice has been shown to be dominated by dimers: the phase diagram contains both strongly resonating, compound spin–orbital dimer states and quasi–static, spin–singlet valence–bond (VB) states. To elucidate the nature of the true ground state in these different regimes, the model is mapped to a number of quantum dimer models (QDMs), each of which has three dimer colors. The generic multicolored QDM, illustrated for the two– and three–color cases, possesses a topological color structure, “color vison” excitations, and broad regions of resonating VB phases. The specific models are analyzed to gain further insight into the likely ground states in the superexchange and direct–exchange limits of the electronic Hamiltonian, and suggest a strong tendency towards VB order in all cases.

PACS numbers: 75.10.Jm, 05.30.-d, 05.50.+q, 71.10.Fd

I. INTRODUCTION

Spin–orbital models have become a very active field of research in the quest for exotic states of matter and novel properties in systems with coupled charge, spin, and orbital degrees of freedom. In real materials, each class of active orbital, lattice structure, and extent of electron filling leads to a different set of problems. An overview of this fabulous wealth of possibilities, focusing on undoped systems and including a complete review of relevant materials, may be found in Ref. [1].

Among these many models, one of the most exotic and mysterious is the triangular–lattice t_{2g} spin–orbital model considered in Ref. [1]. By this is meant the insulating system with a single, fully localized electron on each lattice site, and occupying one of the threefold–degenerate t_{2g} orbitals, a situation which would be realized, for example, in undistorted NaTiO₂ or, with holes, in CoO₂. Depending on which orbitals they occupy, the particles have both superexchange and direct–exchange interactions whose ratio is *a priori* unknown, but it was shown¹ that different types of bond dimer state of the spin and orbital degrees of freedom are favored very strongly for all values of this ratio. The resulting, very rich, phase diagram of possible states includes candidate resonating valence–bond (RVB) states in the limit of pure superexchange interactions and, in the direct–exchange limit, candidate systems for extremely subtle order–by–disorder selection of special valence–bond crystal (VBC) states from very highly degenerate manifolds of dimer coverings.

The question left unanswered despite the extensive energetic studies and plausibility arguments in Ref. [1] was whether one could gain more explicit indications for the suggested unconventional nature of the true ground state in either of these cases. The exotic phenomena which are known from simplified models of highly frustrated and degenerate systems include true liquid phases with no unbroken symmetry in the ground state, topological sec-

tors and excitations, and fractionalization and deconfinement of elementary spinon–type quasiparticles. Given the exhaustive search for both experimental and theoretical realizations of such phenomena in real, electronic systems, the triangular–lattice t_{2g} spin–orbital model is clearly a prime candidate for further investigation. Here it can be noted that the preponderance of evidence in favor of RVB states suggests further that the candidate (spin–orbital) liquid phase is gapped, and hence would have only short–ranged correlation functions and massive, fractional spinon–orbiton excitations. The aim of this study is to approach the unanswered questions through effective quantum dimer models (QDMs).

A review of QDMs, including their origin, properties, and rich associated physics, can be found in Ref. [2]. For the present purposes, specifically pursuing the tantalizing prospect of an RVB state in a real electronic system, the agenda is that laid out as a practical prescription in Ref. [3], namely to map the starting Hamiltonian to the triangular–lattice QDM. In the original QDM exposition of Rokhsar and Kivelson,⁴ it was shown for the square lattice that an exact RVB state exists at one point in the phase diagram (henceforth an “RK point”), and it was later found⁵ that the same model on the triangular lattice allows a rigorous proof for the existence of a true RVB phase with gapped spinon excitations over a finite regime of parameter space. This therefore offers not only a finite chance of any given model having the appropriate energetics, but also an approach which captures automatically the topological criteria associated with RVB physics.

The generic QDM phase diagram² nevertheless contains RVB states over at best a rather narrow range of parameters. Its bulk is occupied by static “columnar” and “staggered” dimer regimes, which respectively maximize or minimize the number of active four–site units, or by other possibilities with a more complex breaking of translational symmetry on generalized plaquettes. Thus the same approach can also be adopted for the direct–exchange limit of the starting model,¹ not in this case

with intent to find an RVB phase, but with a view to isolating the leading fluctuation term which might be responsible for selecting one, or a set of, dimer coverings which are more energetically favorable, through the quantum fluctuations they allow, than all others.

Because QDMs are in general highly simplified, any mapping from a realistic Hamiltonian discards of necessity many degrees of freedom, and thus there is no systematic procedure for their derivation. When proceeding from real, $S = 1/2$, spin-singlet dimers, an immediate dichotomy arises between the definition of QDM states as mutually orthogonal and the fact that no conventional spin-dimer states are orthogonal (the overlap factor being trivially $1/\sqrt{2}$ per site). This non-orthogonality problem is strongly reduced in the triangular-lattice t_{2g} spin-orbital model, and entirely absent in its direct-exchange limit, for reasons which will become apparent in Sec. II. However, this fact also forbids the type of dimer overlap expansion exploited in Ref. [4], and mandates instead a process which proceeds directly from the electronic Hamiltonian. The process of deriving an effective QDM from an orbitally degenerate electronic Hamiltonian was followed in Ref. [6], in the course of an analysis of LiNiO_2 (a system of e_g electrons on a triangular lattice), and while the rationale is similar here, the orthogonality of dimer coverings requires an approach somewhat different in detail.

As a foretaste of the results to follow, in the superexchange limit one finds two different types of “three-color” QDM. The individual dimers are either spin singlets with three different flavors corresponding to the triplet states of the orbitals (ss/ot), or orbital singlets with a conventional spin-triplet flavor (os/st). In both cases, the 9×9 t and v matrices of the QDM reflect the strong breaking of translational and rotational symmetry associated with the consideration of four-site plaquette units in the definition of the QDM. In the former case this drives a lifting of degeneracy in favor of the $T_z = \pm 1$ components of the orbital triplet, while in the latter the spin-triplet dimers may continue to interchange their flavors.

In the direct-exchange limit, there is no mixing between two pairs of dimers on a plaquette, and both the t and v terms of the conventional QDM are identically zero; this rigid locking of dimer color to lattice direction means that the effective model reduces to the one-color variant. The relevant QDM capturing the lowest-order dimer resonance processes is in fact one defined on six-bond triangular loops. While this model dictates a specific ground state, selected from the extensively degenerate manifold of dimer coverings, it does not exclude the possibility of a type of one-dimensional physics¹ where the character of short, fluctuating segments of frustration-decoupled spin chains persists despite the high site coordination of the triangular lattice.

Finally, it should be stressed that none of the physics discussed here is to be confused with that of the “spin-orbital liquid” and “spin-orbital singlet” states introduced recently in Ref. [7]. The work of these authors de-

pends intrinsically on a strong spin-orbit coupling interaction $\lambda_0 \vec{L} \cdot \vec{S}$, and should perhaps therefore be referred to more strictly as “(spin-orbital) physics”. In the present study, which follows a line dating back to the seminal work of Kugel’ and Khomskii,⁸ the terminology “spin-orbital” refers only to the connection, dictated precisely by the electronic Hamiltonian, between the magnetic exchange interactions and the orbital state of each ion, with λ_0 assumed to be negligible. While this approximation is usually taken to be reasonable for $3d$ ions, λ_0 may indeed become important when the physics of the system depends sensitively on the lifting of high degeneracies.

The structure of this manuscript is as follows. The triangular-lattice t_{2g} spin-orbital model is presented in Sec. II, in the form of a minimal review of the contents of Ref. [1] required as a basis for the current analysis. The orthogonality of electronic states with different spin or orbital colors (colored dimers) is demonstrated and the derivation of appropriate QDMs outlined. In Sec. III, the generic multicolored QDM is defined and its properties are studied, illustrating the circumstances under which the color degree of freedom leads to additional topological sectors, possibilities for RK points and RVB ground states, and “color vison” excitations associated with the topological properties. Section IV returns to a detailed analysis of the specific QDMs deduced for the three cases of most interest here, namely (ss/ot) and (os/st) dimers in the superexchange limit and spin-singlet dimers in the direct-exchange limit. A short discussion and summary are presented in Sec. V.

II. MODEL

The derivation begins with the Hubbard Hamiltonian for t_{2g} electrons hopping on a triangular lattice, usually realized on the $\langle 111 \rangle$ planes of a cubic, perovskite-based structure whose local symmetry preserves the orbital degeneracy. The geometry of the system is summarized in Fig. 1, and the average filling of 1 electron per site corresponds to Ti^{3+} or V^{4+} ions. To avoid undue repetition of published material, only the minimal numbers of equations and explanations required for a self-consistent presentation are included here; the reader wishing a complete exposition is requested to consult Ref. [1].

Specializing immediately to a magnetic insulator with on-site repulsion U much greater than the diagonal and off-diagonal (in orbital “color”) electronic hopping integrals, respectively t'_e and t_e , the site occupation is strictly $n_{ia} + n_{ib} + n_{ic} = 1$. The orbitals have a direct connection to the specific lattice directions, and in Fig. 1 the color red for the d_{yz} orbital, is associated with a , green (d_{xz}) with b , and blue (d_{xy}) with c . At second order in a perturbative treatment, the magnetic Hamiltonian can be written in the schematic form

$$\mathcal{H} = J_s \mathcal{H}_s + J_m \mathcal{H}_m + J_d \mathcal{H}_d, \quad (1)$$

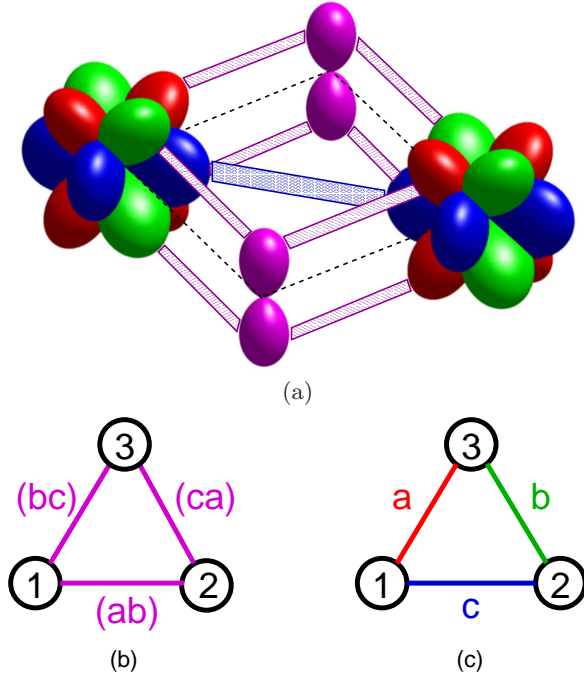


FIG. 1: (color online) (a) Schematic representation of hopping processes for t_{2g} electrons in triangular geometry which contribute to magnetic interactions on a representative (c -axis) bond $\langle ij \rangle$. The orbitals are represented by different colors (greyscale intensities). Superexchange processes involve O $2p_z$ orbitals (violet), and couple pairs of a and b orbitals (red, green) with effective hopping elements t_e , interchanging their orbital color. Direct hopping elements c orbitals (blue) with hopping strength t'_e . (b) Pairs of t_{2g} orbitals active in superexchange and (c) single orbitals active in direct exchange; horizontal bonds correspond to the situation depicted in panel (a).

where

$$J_s = \frac{4t_e^2}{U}, \quad J_m = \frac{4t_e t'_e}{U}, \quad J_d = \frac{4t_e'^2}{U}. \quad (2)$$

Superexchange contributions to \mathcal{H} can be expressed in the form

$$\begin{aligned} \mathcal{H}_s = \frac{1}{2} \sum_{\langle ij \rangle || \gamma} \left\{ r_1 \left(\vec{S}_i \cdot \vec{S}_j + \frac{3}{4} \right) \left[A_{ij}^\gamma + \frac{1}{2} (n_{i\gamma} + n_{j\gamma}) - 1 \right] \right. \\ \left. + r_2 \left(\vec{S}_i \cdot \vec{S}_j - \frac{1}{4} \right) \left[A_{ij}^\gamma - \frac{1}{2} (n_{i\gamma} + n_{j\gamma}) + 1 \right] \right. \\ \left. - \frac{2}{3} (r_2 - r_3) \left(\vec{S}_i \cdot \vec{S}_j - \frac{1}{4} \right) B_{ij}^\gamma \right\}, \quad (3) \end{aligned}$$

where the coefficients

$$r_1 = \frac{1}{1 - 3\eta}, \quad r_2 = \frac{1}{1 - \eta}, \quad r_3 = \frac{1}{1 + 2\eta}, \quad (4)$$

are dictated by the different possible energy states of the virtual $d_i^1 d_j^1 \rightleftharpoons d_i^2 d_j^0$ excitation, which are determined by the Hund coupling $J_H = \eta U$. In real $3d$ transition-metal

ions, η is of order 0.10–0.15. Under a local transformation which takes account of the color-exchanging nature of the superexchange hopping processes,

$$A_{ij}^\gamma = 2 \left(\vec{T}_{i\gamma} \cdot \vec{T}_{j\gamma} + \frac{1}{4} n_i^\gamma n_j^\gamma \right), \quad (5)$$

$$B_{ij}^\gamma = 2 \left(\vec{T}_{i\gamma} \times \vec{T}_{j\gamma} + \frac{1}{4} n_i^\gamma n_j^\gamma \right), \quad (6)$$

where the scalar product in A_{ij} is the conventional expression for pseudospin-1/2 variables and the cross product in B_{ij} is defined as

$$\vec{T}_{i\gamma} \times \vec{T}_{j\gamma} = \frac{1}{2} (T_{i\gamma}^+ T_{j\gamma}^+ + T_{i\gamma}^- T_{j\gamma}^-) + T_{i\gamma}^z T_{j\gamma}^z. \quad (7)$$

Contributions of the form B_{ij} vanish as $\eta \rightarrow 0$ (3). In these expressions, n_i^γ denotes the number of superexchange-active electrons (those able to hop on the bond in question) and $n_{i\gamma}$ the number of superexchange-inactive electrons (which, however, are active in direct-exchange processes): thus the pseudospin scalar and vector product interactions are relevant only when the electrons on both sites are active, while situations with only one active orbital still give nontrivial, spin-dependent contributions.

It is clear that the superexchange contribution on a single bond is minimized either by an orbital-singlet, spin-triplet state, or by a spin-singlet, orbital-triplet state [henceforth (os/st) and (ss/ot)]. Their energies

$$E_{(os/st)} = -Jr_1, \quad (8)$$

$$E_{(ss/ot)} = -\frac{1}{3} J (2r_2 + r_3), \quad (9)$$

are degenerate for $\eta = 0$, while the (os/st) state is favored for finite η . Because the superexchange hopping term is off-diagonal, the orbital singlet is the state

$$|\psi_{os}\rangle = \frac{1}{\sqrt{2}} (|aa\rangle - |bb\rangle), \quad (10)$$

in the original electronic basis, while the orbital triplets are

$$|\psi_{ot+}\rangle = |ab\rangle, \quad (11)$$

$$|\psi_{ot0}\rangle = \frac{1}{\sqrt{2}} (|aa\rangle + |bb\rangle), \quad (12)$$

$$|\psi_{ot-}\rangle = |ba\rangle. \quad (13)$$

Contributions from direct-exchange processes take the form

$$\begin{aligned} \mathcal{H}_d = \frac{1}{4} \sum_{\langle ij \rangle || \gamma} \left\{ \left[-r_1 \left(\vec{S}_i \cdot \vec{S}_j + \frac{3}{4} \right) + r_2 \left(\vec{S}_i \cdot \vec{S}_j - \frac{1}{4} \right) \right] \right. \\ \left. \times \left[n_{i\gamma} (1 - n_{j\gamma}) + (1 - n_{i\gamma}) n_{j\gamma} \right] \right. \\ \left. + \frac{1}{3} (2r_2 + r_3) \left(\vec{S}_i \cdot \vec{S}_j - \frac{1}{4} \right) 4n_{i\gamma} n_{j\gamma} \right\}, \quad (14) \end{aligned}$$

where it is clear once again that far the most favorable energies are obtained from dimer states, but only those creating spin singlets from two electrons with the bond color. Expressions for H_m can be found in Ref. [1], but, as explained there, the very different nature of the two types of singlet state mean that H_m has a qualitative effect on the physics of the system only in rare situations.

Before analyzing the model in more detail, it is necessary to delimit the parameter space of interest to this study, and also to make one essential and completely general comment concerning dimer states of colored electrons. First, the focus of this manuscript is only the two limits of pure superexchange and purely direct exchange. In the superexchange limit, only the regimes with Hund coupling ratio $\eta = 0$ and with physical values $\eta \sim 0.1$ (which is “large” in a sense to be made explicit below), will be considered. In the direct-exchange limit, only $\eta = 0$ is of interest in the context of QDMs: the physics of dimer-based models is determined by purely static contributions at any finite η ,⁹ and changes away from dimer-based states only at the unrealistically large value $\eta = 0.2$. Thus there are three situations to elucidate, all of which have already been shown to be dominated by dimer formation. This restriction is made partly for reasons of practicality, partly to concentrate on the essentially different physics of the differing limits, and partly as a consequence of the above observation concerning the irrelevance of H_m and absence of meaningful mixed processes.

A. Effective dimer overlap

As noted above, a serious problem in mapping real spin models to QDMs is the “non-orthogonality catastrophe,” the fact that all dimer coverings $|c\rangle$ have finite overlap with all others. This is a significant impediment to many forms of both analytical and numerical progress. For $S = 1/2$ entities forming bond spin-singlet states, the generic overlap of two singlets at the same site is simply the prefactor of the singlet wave function, $\alpha = 1/\sqrt{2}$. In the present context, the most meaningful calculation involving α is to consider the overlap of the wave functions of two “horizontal” and two “vertical” $SU(2)$ spin singlets on a four-site plaquette, where it is easy to show from the common elements of $|h\rangle = \alpha^2(|1\uparrow 2\downarrow\rangle - |1\downarrow 2\uparrow\rangle)(|4\uparrow 3\downarrow\rangle - |4\downarrow 3\uparrow\rangle)$ and $|v\rangle = \alpha^2(|4\uparrow 1\downarrow\rangle - |4\downarrow 1\uparrow\rangle)(|3\uparrow 2\downarrow\rangle - |3\downarrow 2\uparrow\rangle)$ that $o = \langle h|v\rangle = 2\alpha^4 = 1/2$.

The single most important generic feature of raising the number of dimer colors, noted already in the context of $1/N$ expansions,² is expected to be that α is reduced, perhaps by a power. However, this hypothesis is dependent on the model, and for a model such as the current one, where electron orbital color sectors change with bond direction, the overlap matrix is not uniform, and in some cases is identically zero. For the three cases of interest here, this can be shown very simply by repeating

the exercise above for (os/st), (ss/ot), and (ss/ $\gamma\gamma$) units, where γ indicates the bond color. For each of the two spin-orbital triplet cases there are nine possible overlap matrix elements to consider, not all of which will be illustrated explicitly. Taking a plaquette of parallel a and c sides, one has

$$\begin{aligned}
|h_{++}(\text{os/st})\rangle &= \alpha^2(|1r\uparrow 2r\uparrow\rangle - |1g\uparrow 2g\uparrow\rangle) \\
&\quad \times (|4r\uparrow 3r\uparrow\rangle - |4g\uparrow 3g\uparrow\rangle), \\
|v_{++}(\text{os/st})\rangle &= \alpha^2(|4g\uparrow 1g\uparrow\rangle - |4b\uparrow 1b\uparrow\rangle) \\
&\quad \times (|3g\uparrow 2g\uparrow\rangle - |3b\uparrow 2b\uparrow\rangle), \\
|h_{00}(\text{os/st})\rangle &= \alpha^4(|1r\uparrow 2r\downarrow\rangle + |1r\downarrow 2r\uparrow\rangle \\
&\quad - |1g\uparrow 2g\downarrow\rangle - |1g\downarrow 2g\uparrow\rangle) \\
&\quad \times (|4r\uparrow 3r\downarrow\rangle + |4r\downarrow 3r\uparrow\rangle \\
&\quad - |4g\uparrow 3g\downarrow\rangle - |4g\downarrow 3g\uparrow\rangle), \\
|v_{00}(\text{os/st})\rangle &= \alpha^4(|4g\uparrow 1g\downarrow\rangle + |4g\downarrow 1g\uparrow\rangle \\
&\quad - |4b\uparrow 1b\downarrow\rangle - |4b\downarrow 1b\uparrow\rangle) \\
&\quad \times (|3g\uparrow 2g\downarrow\rangle + |3g\downarrow 2g\uparrow\rangle \\
&\quad - |3b\uparrow 2b\downarrow\rangle - |3b\downarrow 2b\uparrow\rangle), \\
|h_{++}(\text{ss/ot})\rangle &= \alpha^2(|1r\uparrow 2g\downarrow\rangle - |1r\downarrow 2g\uparrow\rangle) \\
&\quad \times (|4r\uparrow 3g\downarrow\rangle - |4g\downarrow 3g\uparrow\rangle), \\
|v_{++}(\text{ss/ot})\rangle &= \alpha^2(|4g\uparrow 1b\downarrow\rangle - |4g\downarrow 1b\uparrow\rangle) \\
&\quad \times (|3g\uparrow 2b\downarrow\rangle - |3g\downarrow 2b\uparrow\rangle), \\
|h_{00}(\text{ss/ot})\rangle &= \alpha^4(|1r\uparrow 2r\downarrow\rangle - |1r\downarrow 2r\uparrow\rangle \\
&\quad + |1g\uparrow 2g\downarrow\rangle - |1g\downarrow 2g\uparrow\rangle) \\
&\quad \times (|4r\uparrow 3r\downarrow\rangle - |4r\downarrow 3r\uparrow\rangle \\
&\quad + |4g\uparrow 3g\downarrow\rangle - |4g\downarrow 3g\uparrow\rangle), \\
|v_{00}(\text{ss/ot})\rangle &= \alpha^4(|4g\uparrow 1g\downarrow\rangle - |4g\downarrow 1g\uparrow\rangle \\
&\quad + |4b\uparrow 1b\downarrow\rangle - |4b\downarrow 1b\uparrow\rangle) \\
&\quad \times (|3g\uparrow 2g\downarrow\rangle - |3g\downarrow 2g\uparrow\rangle \\
&\quad + |3b\uparrow 2b\downarrow\rangle - |3b\downarrow 2b\uparrow\rangle), \\
|h(\text{ss/cc})\rangle &= \alpha^2(|1b\uparrow 2b\downarrow\rangle - |1b\downarrow 2b\uparrow\rangle) \\
&\quad \times (|4b\uparrow 3b\downarrow\rangle - |4b\downarrow 3b\uparrow\rangle), \\
|v(\text{ss/aa})\rangle &= \alpha^2(|4r\uparrow 1r\downarrow\rangle - |4r\downarrow 1r\uparrow\rangle) \\
&\quad \times (|3r\uparrow 2r\downarrow\rangle - |3r\downarrow 2r\uparrow\rangle),
\end{aligned}$$

and similarly, whence

$$\begin{aligned}
o_{+,+,+}(\text{os/st}) &= o_{-,-,-}(\text{os/st}) = \alpha^4 = 1/4, \\
o_{+,0,+}(\text{os/st}) &= o_{+0,0+}(\text{os/st}) = \alpha^6 = 1/8, \\
o_{0+,0+}(\text{os/st}) &= o_{0+,+0}(\text{os/st}) = \alpha^6 = 1/8, \\
o_{00,00}(\text{os/st}) &= 2\alpha^8 = 1/8, \\
o_{0-,0-}(\text{os/st}) &= o_{0-,-0}(\text{os/st}) = \alpha^6 = 1/8, \\
o_{-,0,-}(\text{os/st}) &= o_{-,0,0-}(\text{os/st}) = \alpha^6 = 1/8, \\
o_{\mu\nu,\rho\sigma}(\text{os/st}) &= 0 \quad \text{otherwise}, \\
o_{00,00}(\text{ss/ot}) &= 2\alpha^8 = 1/8, \\
o_{\mu\nu,\rho\sigma}(\text{ss/ot}) &= 0 \quad \text{otherwise}, \\
o(\text{ss}/\gamma\gamma) &= 0.
\end{aligned} \tag{15}$$

For (os/st) dimers there are finite overlap matrix ele-

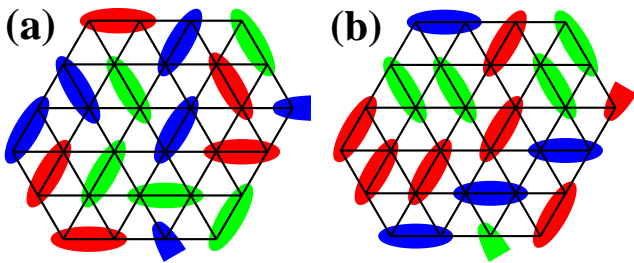


FIG. 2: (color online) QDM representations. (a) Three-color QDM as obtained in the superexchange limit for both (ss/ot) and (os/st) dimers; dimers of any color may occupy any bond, but not all processes (t or v) may be allowed on plaquettes containing two dimers. Dimer colors do not correspond to the colors in Fig. 1. (b) QDM obtained in the direct-exchange limit for (ss/ $\gamma\gamma$) dimers, whose colors do correspond to those in Fig. 1. Bonds of the three different orientations have only one color each, and thus the color is no longer a degree of freedom. This defines an effective one-color QDM.

ments within each S_z sector, all (but one) of considerably higher order than the conventional spin-singlet problem. However, the 9×9 overlap matrix is rather sparse. For (ss/ot) dimers, the orbital color combinations forbid any overlap matrix elements other than for pairs of $T_z = 0$ dimers. For bond-colored, spin-singlet dimers there are no overlap matrix elements at all. Thus the highly non-uniform nature of the matrix elements in the superexchange model and the fact that they vanish in the direct-exchange model preclude any sort of meaningful expansion in the inverse of the overlap matrix.⁴ As noted in Sec. I, the matrix elements t and v of the relevant QDMs will instead be deduced directly at second-order in perturbation theory using the electronic Hamiltonian.

B. Superexchange model

In the limit $\eta = 0$, the bond Hamiltonian of Eq. (3) takes the more transparent form

$$\mathcal{H}_{s0} = J_s \sum_{\langle ij \rangle \| \gamma} 2 \left(\vec{S}_i \cdot \vec{S}_j + \frac{1}{4} \right) \left(\vec{T}_{i\gamma} \cdot \vec{T}_{j\gamma} + \frac{1}{4} n_i^\gamma n_j^\gamma \right) + \frac{1}{2} (n_{i\gamma} + n_{j\gamma}) - \frac{1}{2}. \quad (16)$$

The six-fold single-bond degeneracy of (ss/ot) and (os/st) dimers is lifted in favor of the former by quantum fluctuations on the off-dimer bonds at $\eta = 0$,¹ leaving a threefold degeneracy corresponding to the orbital triplet states of the two electrons, $T_z = 1, 0$, and -1 . Thus one expects a QDM with three different flavors of dimer, a situation depicted in Fig. 2(a). Note that these “colors” are not the same as the spectral colors in Fig. 1, which are associated directly with the symmetry of the t_{2g} levels, but correspond to three possible orbital states on each bond of a given direction [Eqs. (11)–(13)]. The

three analogous states for a different lattice direction are composed of a different t_{2g} -color pair.

However, for physical values of η around 0.1, the (os/st) dimers are preferred as the direct lifting of degeneracy in the one-bond Hamiltonian outweighs the kinetic effects. This regime is delimited by a lower bound, which for the four-site cluster is $\eta_l = 0.03$, and an upper bound of $\eta_u \sim 0.15$ where the ground state becomes ferromagnetic by a lifting of the spin-triplet degeneracy.¹ Within this range, one has a three-color QDM similar to the (ss/ot) case [Fig. 2(a)], but one in which the colors correspond to the spin triplet states of the two electrons, $S_z = 1, 0$, and -1 . The triplet states in the spin sector are the same for every bond direction, and this fact is responsible for the differences from the (ss/ot) situation observed already in the overlap matrix elements. The QDM matrix elements can also be expected to differ in several respects.

Summarizing the situation to this point, in the superexchange limit of the model one has a number of energetic criteria which can be compared to the RVB criteria of Ref. [3]. The former are¹ (i) a very strong tendency to dimer formation, (ii) a large semi-classical degeneracy of basis states, namely the set of coverings formed from these dimers, and (iii) that resonance processes on four-site plaquette units provide a significant energetic contribution. From (iii), a minimal triangular-lattice QDM should in principle contain, within the dimer-flipping term t and the static pair term v , the leading corrections to the static VB energy (determined by J_s). The question is then reduced to whether the regime $t/v \gtrsim 1$ of RVB physics⁵ can be attained.

C. Direct-exchange model

Here only the $\eta = 0$ limit of the model,

$$\mathcal{H}_{d0} = J_d \sum_{\langle ij \rangle \| \gamma} \left(\vec{S}_i \cdot \vec{S}_j - \frac{1}{4} \right) n_{i\gamma} n_{j\gamma} - \frac{1}{4} \left(n_{i\gamma} (1 - n_{j\gamma}) + (1 - n_{i\gamma}) n_{j\gamma} \right), \quad (17)$$

will be considered. As noted above, the spin-singlet state optimizing the bond energy can be formed only from two electrons of the bond color. Thus the three apparent t_{2g} colors of the dimers are locked rigidly to the bond direction, with no finite matrix elements for directional fluctuations, a situation depicted in Fig. 2(b). The effective QDM will then be equivalent to a one-color model.

In addition to the studies of Ref. [1], this model has also been considered in some detail by Jackeli and Ivanov.⁹ These authors demonstrated that the extensively degenerate manifold of (bond-colored) dimer coverings forms a set of exact eigenstates of the second-order Hamiltonian. In deducing the leading perturbations which would select a type of order, they allowed finite values of J_H , which lead at order η^3 to a ferromagnetic interaction on inter-dimer bonds with one (but not two) dimers of the bond

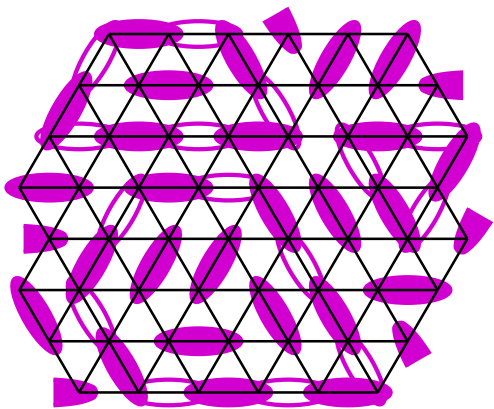


FIG. 3: (color online) Representation of allowed dimer fluctuation processes in the direct-exchange limit, shown for a system of only one dimer color. These processes define loops whose sides have even numbers of bonds, and which (to maintain complete dimer covering of the lattice) must enclose an even number of sites. Illustrated are the lowest three loops, which have lengths of 6, 10, and 14 bonds.

color. As a result, particular static dimer configurations are selected (the type of state is unique, albeit with a translational and rotational degeneracy of 60), but there remains no contribution from the positional resonance of dimers. The aim here is to investigate the consequences of the lowest-order dimer resonance processes of a type which would give valid contributions to a QDM.

In this limit of the model, electrons in dimer singlets may hop only in the direction corresponding to their bond color. Thus virtual processes are highly restricted and the true dimensionality of the system is far lower than the connectivity of the triangular lattice would suggest.¹ Because a four-site plaquette contains no two bonds of the same direction, not only is the overlap matrix element zero (above) but the t and v terms of the conventional, triangular-lattice QDM are also identically zero. A QDM based on higher-order terms will therefore be required. The only kinetic contributions on the triangular lattice are given by paths of even side-lengths, and which enclose even numbers of sites. Some valid loops are shown in Fig. 3. Here the contributions t' and v' from fluctuation processes on six-bond triangles will be computed, while the leading perturbations from higher allowed loops (the 10-bond trapezium and 14-bond irregular pentagon) can be argued to be small. The ground state of the resulting t' - v' QDM should contain the leading effects of dimer resonance processes on the highly degenerate manifold of static VB coverings.¹ One may then also consider whether the energy of this state is more favorable than the spontaneous one-dimensionalization of the system into effectively decoupled Heisenberg chains of a single orbital color. This outcome, the lowest-energy possibility found in Ref. [1], is generally held to be rather unlikely, although from the 1D nature of the electronic processes in this limit of the model it is not entirely im-

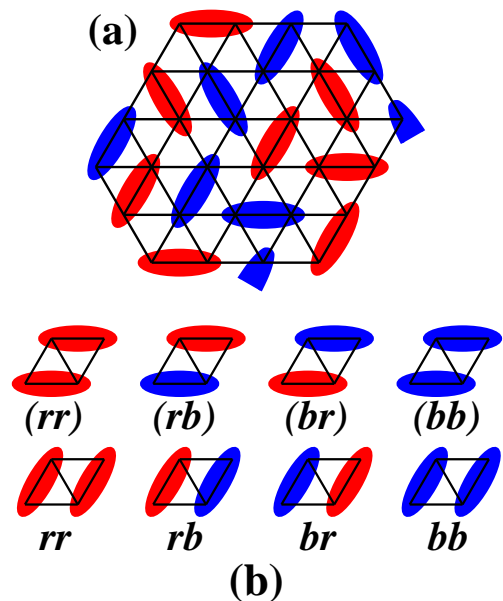


FIG. 4: (color online) (a) Dimer covering of the two-color QDM on the triangular lattice. (b) Representation of the eight possible configurations of two colored dimers on a flip-flop (ac) plaquette.

plausible.

Commenting briefly on further models which may arise within the t_{2g} system on the triangular lattice, clearly there are many of these even at unit filling per site. The entire range $0 < J'/J < \infty$ is of obvious physical importance, and in principle presents a model with four types of dimer. However, the lack of symmetry between the two limits implies automatic selection effects which will favor a smaller number of these dimers (those maximizing virtual kinetic processes). The results of Ref. [1] suggest a first-order transition from the superexchange regime (QDMs with up to three colors) to the direct-exchange regime (a one-color QDM) at an intermediate value of J'/J but with no intermediate phase. A second possibility is the regime of very high η , where for all values of J'/J the preference for dimers will melt, and one obtains very highly degenerate sets of color configurations among which the (now subdominant) Heisenberg interactions are responsible for selection effects.

To conclude this section, specific colored QDMs can be obtained for the three cases of interest and, within the approximations inherent in the derivation process (by which is meant the breaking of translational symmetry and the discarding of very many degrees of freedom), all are expected to yield additional information concerning the physics of the ground state of the starting electronic Hamiltonian. Before proceeding to a detailed analysis of these models (Sec. IV), it is necessary to consider the physical possibilities contained within QDMs possessing an additional color degree of freedom.

III. GENERAL COLORED QDM

Consider a QDM on the triangular lattice with two different types of dimer, which will be labeled by the colors red and blue. An arbitrarily chosen dimer covering is shown in Fig. 4(a). To systematize the description of this system, one begins by noting that there are eight possible states on each rhombic plaquette: taking an (ac) plaquette for illustration [Fig. 4(b)], let these be denoted by $i = rr, rb, br,$ and bb for pairs of a -axis dimers and $(rr), (rb), (br),$ and (bb) for pairs of c -axis dimers. The QDM Hamiltonian has the form

$$H = \sum_{\gamma=1}^3 \sum_{i=1}^{2N} H_p \quad (18)$$

where there are $2N$ plaquettes of any one orientation for a system of $2N$ sites (N dimers), and γ labels the three plaquette orientations on the triangular lattice. The plaquette Hamiltonian is given by

$$\begin{aligned} H_p = & -t_{rr,rr} (|\langle \text{red/red} \rangle\rangle \langle \text{red/red} | + |\langle \text{red/blue} \rangle\rangle \langle \text{red/blue} |) \\ & -t_{rr,rb} (|\langle \text{red/red} \rangle\rangle \langle \text{red/blue} | + |\langle \text{red/blue} \rangle\rangle \langle \text{red/red} |) \\ & -t_{rr,rb} (|\langle \text{red/blue} \rangle\rangle \langle \text{red/blue} | + |\langle \text{red/red} \rangle\rangle \langle \text{red/red} |) + \dots \\ & -t_{rb,br} (|\langle \text{red/blue} \rangle\rangle \langle \text{red/blue} | + |\langle \text{red/blue} \rangle\rangle \langle \text{red/red} |) \\ & -t_{rb,br} (|\langle \text{red/blue} \rangle\rangle \langle \text{red/blue} | + |\langle \text{red/blue} \rangle\rangle \langle \text{red/red} |) + \dots \\ & +v_{rr,rr} (|\langle \text{red/red} \rangle\rangle \langle \text{red/red} | + |\langle \text{red/blue} \rangle\rangle \langle \text{red/blue} |) \\ & +v_{rr,rb} (|\langle \text{red/red} \rangle\rangle \langle \text{red/blue} | + |\langle \text{red/blue} \rangle\rangle \langle \text{red/blue} |) + \dots \\ & +v_{br,bb} (|\langle \text{red/blue} \rangle\rangle \langle \text{red/blue} | + |\langle \text{red/blue} \rangle\rangle \langle \text{red/blue} |) + \dots \end{aligned}$$

and thus is represented by an 8×8 matrix acting on the state vector $[rr, rb, br, bb, (rr), (rb), (br), (bb)]$. This matrix has a “diagonal block” v_{ij} and off-diagonal blocks t_{ij} and t_{ij}^* . The 4×4 v_{ij} matrix specifies the static energies of the $rr, rb, br,$ and bb configurations, and the assumption of plaquette symmetry between a - and c -axis dimer pairs, enforced here, means that this symmetric matrix also defines the analogous energies for $(rr), (rb), (br),$ and (bb) . The 4×4 t_{ij} matrix specifies the flipping energies of $rr, rb, br,$ and bb into $(rr), (rb), (br),$ and (bb) , and conversely; the symmetry $t_{i(j)} = t_{(j)i}$ (Hermitian conjugation) ensures that H_{ij} is a symmetric matrix and the symmetry $t_{i(j)} = t_{i(j)}$ (one-plaquette axis permutation) ensures further that t_{ij} is symmetric. Thus the brackets are redundant in the labels of v_{ij} and t_{ij} .

The nature of the two-color triangular-lattice QDM depends on the matrix elements of v_{ij} and t_{ij} , which could in principle vary between the limits

$$\begin{aligned} v_{ij} &= v[1, 0, 0, 0; 0, 0, 0, 0; 0, 0, 0, 0; 0, 0, 0, 1], \\ t_{ij} &= t[1, 0, 0, 0; 0, 0, 0, 0; 0, 0, 0, 0; 0, 0, 0, 1], \quad (19) \end{aligned}$$

and

$$\begin{aligned} v_{ij} &= v[1, 1, 1, 1; 1, 1, 1, 1; 1, 1, 1, 1; 1, 1, 1, 1], \\ t_{ij} &= t[1, 1, 1, 1; 1, 1, 1, 1; 1, 1, 1, 1; 1, 1, 1, 1]. \quad (20) \end{aligned}$$

The system represented by Eqs. (19) is one where potential and kinetic energy are gained only on plaquettes containing two dimers of the same color, and hence this is a dilute version of the one-color QDM. While some additional symmetries may arise (below) from the conservation of each color individually, the energetics and dynamics of the system appear to be somewhat trivial as a result of the dilution. Equations (20) represent a “color-blind” system where the standard QDM processes occur with the same amplitudes irrespective of dimer color, and is therefore equivalent to a one-color QDM but with a redundant degree of freedom. While it is the signs of the elements of v_{ij} and t_{ij} which are most important in determining the ground state of the model, other than v_{ii} there is in general no need for these to be real, and one could consider matrix elements which have different signs or phase factors occurring in different patterns.

A. Topological structure

One of the most important properties of QDMs is the fact that they display a topological structure (also “topological order”),² which is characterized by the presence of topological invariants and associated gauge symmetries. For a colored QDM it is therefore natural to investigate whether there exists some additional, nontrivial topological structure arising from the presence of the color degree of freedom.

For this one must first recall the origin of the Z_2 gauge symmetry which exists in the conventional QDM. This is ultimately a consequence of the condition that each site must contain only one hard dimer on one of the bonds connected to it. If one considers the number of dimers intersecting an arbitrary line which spans the system, it is this constraint which is responsible for the fact that any dimer-rearrangement process (which defines a loop) can change the number of dimers intersecting the line only in multiples of 2. This property cannot be affected by any set of color matrix elements t_{ij} and v_{ij} within the framework presented above, and therefore this Z_2 symmetry cannot be embedded within some higher symmetry group. Alternatively stated, while it is possible to alter dimer colors without altering the number which intersect the arbitrarily chosen line, it is not possible to alter the number intersecting the line without altering the numbers of dimers of each color which intersect it.

Thus the symmetry of the colored QDM can be at best $Z_2 \otimes G$, where G is a different symmetry group. A number of possibilities could be considered which avoid this hard constraint, including “soft” dimers which must only have unit squared amplitude on the sum of the bonds at a site, multiple dimers per site (for example a representation of

a $S = 1$ spin system), a diluted model with undimerized sites or pairs of sites, and models of quantum trimers or quantum quadrupers on particular lattices and with particular matrix elements analogous to t_{ij} and v_{ij} . While some of these may indeed be constructed to deliver topological structures and gauge symmetries beyond Z_2 , they will not be considered further in the present context.

Returning to a consideration of the number of dimers intersecting an arbitrary line across the system, the quantity $N = N_r + N_b$ (the total numbers of red and blue dimers in the system) is always a constant, while $n_r + n_b$ (the numbers of red and blue dimers intersecting the line) may change only in units of 2. This property defines the four topological sectors on a torus and is reflected in the Z_2 symmetry discussed above.

Nontrivial color sectors are characterized by $n_r - n_b$. This quantity can vary from $-N$ to $+N$ in steps of 2; there are N sectors if N is odd and $N + 1$ if N is even. Thus a trivial color-sector structure, where sectors with $(N_r, N_b) = (K, L)$ are connected to sectors with $(K \pm 1, L \mp 1)$, is characterized by $(n_r - n_b)/2$ changing in steps of 1. Two nontrivial alternatives arise in the two-color QDM.

(i) If the matrices t_{ij} and v_{ij} have the forms $[a, 0, 0, 0; 0, b, c, 0; 0, c, b, 0; 0, 0, 0, d]$, N_r and N_b are conserved individually and $(n_r - n_b)/2$ is a constant. Thus there are N or $N + 1$ topological color sectors which cannot be mixed. The symmetry may be labeled $Z_2 \otimes \mathbf{Z}$. Models with an infinite set of discrete topological invariants labeled by the set of integers \mathbf{Z} constitute a realization of an ensemble of string nets, the theory of which can be found in Ref. [10].

(ii) If the matrices t_{ij} and v_{ij} have the forms $[a, 0, 0, e; 0, b, c, 0; 0, c, b, 0; e, 0, 0, d]$, terms interconverting between two red and two blue dimers are also permitted. In this case, sectors (K, L) are connected to sectors $(K \pm 2, L \mp 2)$ and $(n_r - n_b)/2 \pmod{2}$ is a topological invariant. Sectors (K, L) and $(K \pm 1, L \mp 1)$ have no overlap, and changing the color of a single dimer is a process which results in a topological defect (below), one which cannot be rectified without a string of local processes which extends to the boundary of the system. In this case one has four additional color sectors on a torus, and the symmetry is $Z_2 \otimes Z_2$: one Z_2 is for the hard dimer structure and the other for the color structure.

If further 0 elements in case (ii) were to be made finite, then the Hamiltonian matrix would mix sectors differing by $(n_r - n_b)/2 = 1$, and the trivial topological structure would be restored.

Thus the presence of a dimer color in a QDM can lead to additional topological structure in the color sector.

B. RK points and RVB phases

Another key property of QDMs is the fact that they display Rokhsar–Kivelson (RK) points. A further essential question for colored QDMs therefore concerns the existence of RK points in models described by the different types of matrix above. The RK point of the original QDM occurs at $t = v$. It has the property that the equal-amplitude superposition (with equal phase) of all possible dimer coverings in each topological sector, a “liquid” state with no local order, is the ground state. While on the square lattice there are gapless excitations at the RK point, on the triangular lattice this ground state is completely gapped and the properties of the RK point are preserved across a phase of finite extent. This is the RVB phase.

The equal-amplitude superposition $|\psi\rangle = \frac{1}{\sqrt{N}} \sum_1^{N_c} |c\rangle$, where $|c\rangle$ represents the N_c dimer coverings in the chosen topological sector, has energy $\langle\psi|H|\psi\rangle = (v - t)\langle n^{\text{fl}}\rangle$, where n^{fl} is the number of flippable plaquettes in a covering. To show that this wave function is an eigenstate requires writing the QDM Hamiltonian as a sum of plaquette projectors, which in turn requires the condition $v = t$. At the RK point, the energy is zero, while on the triangular lattice it is negative over a range of values $1 \leq t/v \lesssim 1.3$, beyond which there are transitions to different ground states (of ordered dimers or groups of plaquettes, hence breaking the translational and rotational symmetry of the lattice).

The proof that a more general $|\psi\rangle$ is an eigenstate of a more general QDM Hamiltonian sets the restrictive condition that H must still be expressible as a sum of projectors. In a two-color model of the type considered in this section, where H contains many terms t_{ij} and v_{ij} , the RK condition is that $t_{ij} = v_{ij}$ for each matrix component. The wave function in this case contains all coverings, in each topological sector (where now the color may increase the number of sectors), of dimers of both colors. If this structure is not maintained, $|\psi\rangle$ will not be an eigenstate, but may still be the ground state, and will retain a gap to all excitations up to the boundary of the RVB phase.

The condition that $|\psi\rangle$ be the ground state of H is, up to a point, less strict. The energy of the two-color version of the wave function $|\psi\rangle$ is

$$E = \sum_{ij} g_{ij}(v_{ij} - t_{ij}), \quad (21)$$

where g_{ij} is a statistical factor accounting for the probability of finding each specific plaquette state (here those plaquettes not only containing two dimers but also with a finite matrix element in t_{ij} and/or v_{ij} for processes involving these). In fact $g_{ij} = \langle n_{ij}^{\text{fl}} \rangle$ is the average number of flippable plaquettes of each type in the equal-amplitude superposition. For equal dimer numbers, $N_r = N_b$, in a two-color model, all coefficients g_{ij} are equal, but this is no longer the case if, for example,

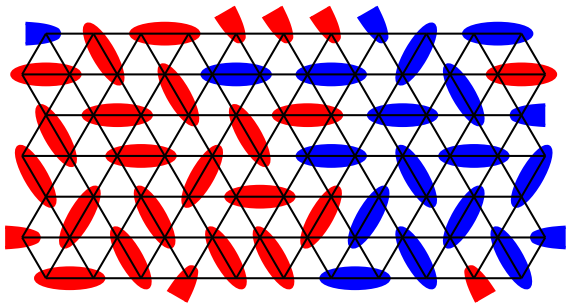


FIG. 5: (color online) Schematic representation of a two-color dimer system undergoing phase separation: if $t_{rr,rr} > v_{rr,rr}$ but $t_{bb,bb} < v_{bb,bb}$, a dynamically driven phase separation will occur (mitigated by larger values of matrix elements mixing with local rb and (rb) states). The “staggered” configuration of the predominantly blue region is static, whereas the red region undergoes local, symmetry-restoring resonance processes.

$N_r \neq N_b$, or if a more complex model defined on a more complex geometry is considered.

The physics of the colored QDM is in this regard not qualitatively different from that of the conventional QDM. The equal-amplitude superposition does not gain a large amount of energy on each plaquette, but it is the ground state because it profits from quantum fluctuations on every single plaquette, and not merely from a symmetry-broken subset of these (which can be at most $1/6$ of the total plaquette number). The freedom to have every component obey $1 \leq t_{ij}/v_{ij} \lesssim 1.3$ clearly defines a relatively broad regime of parameter space: should the ratio stray outside these bounds for some components, the preference of the remaining components for full resonance will act to maintain the RVB phase.

However, in this situation a multicolored QDM is susceptible to phase separation. As a specific but simple example, consider a model with only the terms $v_{rr,rr}$, $v_{bb,bb}$, $t_{rr,rr}$, and $t_{bb,bb}$ (all positive) large, while other matrix elements are finite [to avoid the dilution paralysis problem of Eq. (19)] but very small. The large elements obey $t_{rr,rr} > v_{rr,rr}$ and $t_{bb,bb} < v_{bb,bb}$, whence even if

$$t_{rr,rr} - v_{rr,rr} > v_{bb,bb} - t_{bb,bb}, \quad (22)$$

so that the sum of kinetic terms exceeds that of potential terms, flippable blue plaquettes will entail a local energy cost. This can be avoided if blue dimers tend to adopt a “staggered” phase,⁵ meaning any one of the set of dimer coverings ensuring that there are no flippable blue plaquettes. The transition to the staggered phase in the conventional triangular-lattice QDM is of first order, making the tendency towards phase separation strong. In the meantime, red plaquettes may continue to profit from resonance across a fraction of the system consistent with the ratio N_r/N (Fig. 5), but the wave function is now far from an equal-amplitude superposition of all possibilities. At the opposite boundary of the RVB region, one of the colors could be expected to begin to cluster

in the $\sqrt{12} \times \sqrt{12}$ formation.^{5,11} This phase-separation effect becomes less pronounced as the values of the other matrix elements in H_{ij} (for example contributions from flippable red-blue plaquettes) are increased.

C. Color visons and colored Majorana fermions

The presence of topologically distinct Z_2 color sectors in case (ii) above results in color vison excitations. While local processes contained in the matrix elements of t_{ij} and v_{ij} result in excited states in the same topological sector, some states with very minimal differences can be in different topological sectors. An example in case (ii) is the exchange of color on a single dimer, a process not permitted by the local matrix elements. The (low-lying) excitation which results is topological in nature: to connect the initial and final states requires a string of local processes which spans the system.¹² An alternative, similar to an intermediate stage in the process of “repairing” the topological defect, is the presence of defect pairs, or color visons connected by a finite-length path. These defects are exactly analogous to the conventional Z_2 visons which arise from the dimer positions, but here they are (for a pure color vison, and not a vison of mixed character) present only in the color sector, *i.e.* without altering any dimer positions. Topological excitations will also be present in the \mathbf{Z} color sector, for which the reader is referred to Ref. [10].

Statements about color visons may be made rigorous by formulating a Majorana-fermion representation of the statistical average over the different dimer coverings. Following Ref. [12], the complete ensemble of dimer configurations may be represented by the partition function of a set of real, auxiliary fermionic variables a_l^m corresponding to each lattice site,

$$Z = \int \prod_{l,m} da_l^m \exp\left[\sum_{ll'mm'} a_l^m A_{ll'}^{mm'} a_l^{m'}\right] = \text{Pfaff}(A_{ll'}^{mm'}), \quad (23)$$

where the right-hand side is the Pfaffian of the matrix of effective Majorana-fermion hopping amplitudes on each bond $\langle ll' \rangle$ of the lattice. In the two-color QDM, two colors of Majorana fermion are required for each site, and this is represented in the index m . The matrix elements $A_{ll'}^{mm'}$ take the values ± 1 for neighboring sites l and l' , and 0 otherwise. Hence each bond is described by a 2×2 matrix

$$\overleftrightarrow{A}_{ll'} = \begin{pmatrix} A_{ll'}^{rr} & A_{ll'}^{rb} \\ A_{ll'}^{br} & A_{ll'}^{bb} \end{pmatrix}, \quad (24)$$

which is net antisymmetric under exchange of l and l' ($A_{ll'}^{mm} = -A_{l'l}^{mm}$, $A_{ll'}^{mm'} = -A_{l'l}^{m'm}$). Because all but the sparsest models contain plaquette processes which on any given bond can exchange red and blue dimer ends, and change the number of dimer ends of each color, all matrix elements are finite in the (r, b) basis. The condition which ensures that all dimer coverings appear in the partition

function with the correct relative sign is that the product $\prod_{\Gamma} \overleftrightarrow{A}_{ll'} = -\overleftrightarrow{I}$ on any loop Γ consisting of an even number of bonds $\langle ll' \rangle$: the product of an even number of 2×2 matrices around a plaquette (of 4 to $2N$ sites) should be the negative 2×2 identity. The two -1 terms in $-\overleftrightarrow{I}$ correspond to the two Z_2 sectors in the two-color QDM.

The Pfaffian formulation becomes more transparent on symmetrizing the Majorana fermions,

$$\begin{aligned} a_l^s &= \frac{1}{\sqrt{2}}(a_l^r + a_l^b), \\ a_l^a &= \frac{1}{\sqrt{2}}(a_l^r - a_l^b), \end{aligned} \quad (25)$$

whence $\tilde{A}_{ll'}^{ss} = (A_{ll'}^{rr} + A_{ll'}^{rb} + A_{ll'}^{br} + A_{ll'}^{bb})/2$ and similarly for the other three elements of $\tilde{A}_{ll'}$ in the symmetrized basis. The situation is particularly simple in a color-symmetric problem, by which is meant one with $N_r = N_b$, $v_{rr,rr} = v_{bb,bb}$, and $t_{rr,rr} = t_{bb,bb}$; other situations are qualitatively similar but notationally more complex. In the color-symmetric case, the model is invariant under interchange of the two colors, $r \leftrightarrow b$. Hence $A_{ll'}^{rr} = A_{ll'}^{bb} = A_{ll'}^{mm}$ and $A_{ll'}^{rb} = A_{ll'}^{br} = A_{ll'}^{mm'}$, which leads to

$$\begin{pmatrix} \tilde{A}_{ll'}^{ss} & \tilde{A}_{ll'}^{sa} \\ \tilde{A}_{ll'}^{as} & \tilde{A}_{ll'}^{aa} \end{pmatrix} = \begin{pmatrix} A_{ll'}^{mm} + A_{ll'}^{mm'} & 0 \\ 0 & A_{ll'}^{mm} - A_{ll'}^{mm'} \end{pmatrix}. \quad (26)$$

Thus the bond matrix is diagonal in the $(r+b, r-b)$ basis. The plaquette product then reduces to two products of even numbers of scalars, each of which has value -1 . The upper product corresponds to the (hard-dimer-related) Z_2 symmetry of the conventional one-color model and the lower to the Z_2 symmetry of the color sector.

Defective plaquettes, those where the product is no longer -1 , describe states which do not belong in the same topological sector, and hence are topological defects. Defects in the upper index of the symmetrized bond matrix are conventional visons, while those in the lower index are color visons. While it is difficult (for obvious reasons) to represent a single vison in a finite region of a system, Fig. 6 presents a schematic representation of two color visons connected by a path of finite length. The Z_2 symmetry of the color sector dictates that a vison is its own antivison.

The discussion can be extended in a straightforward manner to three dimer colors. It is important to note first that three colors do not imply a Z_3 symmetry, or indeed anything similar to this. A Z_3 symmetry would require three separate topological sectors for each periodic direction on a cylinder or torus, and no aspect of the purely pairwise interactions in a QDM permits terms creating such a structure; this is not a question of the choice of the matrix elements in t_{ij} and v_{ij} , but one concerning the architecture of the model. With green (g) as the third color, the analogs of cases (i) and (ii) above are rather the following.

- (i3) For interactions conserving the number of dimers of each color, there are $N(N+1)/2$ (for odd N)

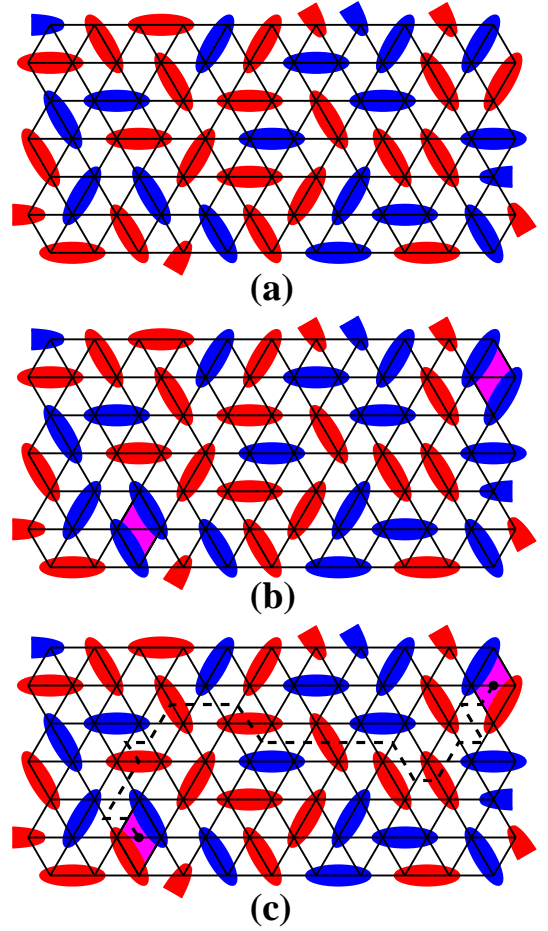


FIG. 6: (color online) (a) Arbitrarily chosen dimer configuration in a two-color QDM. (b) A color vison is introduced in the lower left corner by exchanging the color of a single dimer (here from red to blue) without altering the positions of any dimers of either color. Because this configuration would not be in the same topological color sector as that in panel (a), attempting to restore configuration (a) by applying the local matrix elements of case (ii) results in a path which spans the system. If, however, a second color vison is also present, in the upper right corner, then the vison pair may annihilate. For simplicity, the visons are represented as residing on flippable plaquettes in which the color-exchanged dimer is involved; dealing with color-exchanged dimers not initially on a flippable plaquette is a small extension, and more general considerations can be used to isolate visons as triangle-based entities.¹² (c) One possible path of local processes connecting the two color visons.

or $(N+1)(N+2)/2$ (for even N) separate and unmixed color sectors which would be labeled by $\mathbf{Z} \otimes \mathbf{Z}$.

- (ii3) For interactions conserving the number of dimer colors in each pair modulo 2, there is a set of “three” separate Z_2 subsectors corresponding to $(n_r - n_b)/2$, $(n_b - n_g)/2$ and $(n_g - n_r)/2 \pmod{2}$. One of the three constraints is trivially redundant (a necessary consequence of the other two),

and hence the model has a $Z_2 \otimes Z_2 \otimes Z_2$ topological structure with one hard-dimer sector and two independent Z_2 color sectors.

A Pfaffian formulation of the statistical average over all dimer coverings would require three Majorana fermions per site. In case (ii₃) it would contain one conventional vison plus two types of rgb vison.

IV. TRIANGULAR-LATTICE t_{2g} MODELS

In this section, let $J = 4t_e^2/U$ denote the bare superexchange bond strength (J_s in Sec. II) and $J' = 4t_e'^2/U$ the bare direct-exchange interaction (J_d in Sec. II). Some of the results to follow lie beyond the mean-field Ansatz used in Ref. [1]. All derivations will be restricted to the lowest relevant order in the electronic Hamiltonian. Further matrix elements would naturally be present at higher orders, and although these are small, they may have qualitative effects such as the mixing of color sectors (*i.e.* the introduction of further off-diagonal elements in the QDM matrices).

In the results of this section, the QDM matrix elements v and v' are always negative because all of their even-order contributions are net energy gains. The signs of t and t' depend on the choice of phase for each singlet, and hence on an arrow-direction convention applied to the triangular lattice. These signs are, however, unimportant in the analysis of a QDM, where they are a matter of convention (easily altered by a change of bond phases),⁴ and thus will not be tracked explicitly. In fact the signs of t and t' here, with no further manipulation, are generally positive (bearing in mind the overall minus sign in the QDM definition), because all loops involve even numbers of plaquette edge bonds of the same type. The sign of the ratio t/v is, however, crucial in determining the ground state.

A. Superexchange limit, $\eta = 0$

Here the ground state of the system is composed of (ss/ot) color triplets. As noted in calculating the overlap of different dimer states in Sec. II, this model has quite asymmetric matrix elements due to the breaking of translational symmetry involved in considering four-site plaquette units. This is due specifically to the direct constraint on the orbital space by the choice of plaquette, and hence is stronger for (ss/ot) than for (os/st) dimers.

Consider an (ac) plaquette, as represented in Fig. 7(a). Let the label $+$ denote the state $|rg\rangle$, $-$ the state $|gr\rangle$ and 0 the state $\frac{1}{\sqrt{2}}|rr\rangle + |gg\rangle$ [see Eqs. (11)–(13)]. The allowed electron-hopping processes out of the red-green bond dimers are for green electrons to hop along the c -axis bonds, becoming blue as they do so, and for red electrons to hop along the single b -axis bond, also becoming blue. The change of color on hopping means that

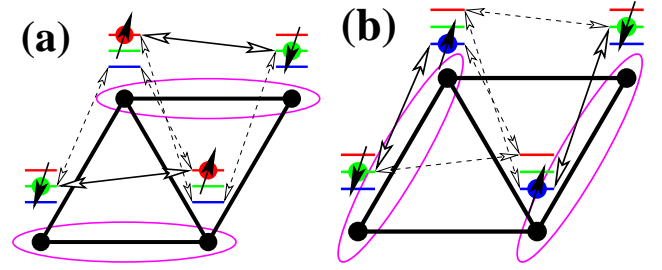


FIG. 7: (color online) Superexchange limit, (ac) plaquette, showing selected (a) horizontal and (b) “vertical” (ss/ot) dimer pairs (magenta ellipses), along with a schematic representation of allowed electron hopping processes. The orbital triplet states are $+ -$ in both panels.

there is no effect of the spin state in blocking possible processes.

For finite elements in the t matrix, the final state must be a pair of spin singlets on the c -axis bonds with green-blue color triplet character, as represented in Fig. 7(b). Somewhat surprisingly, there exists precisely one second-order process which achieves this, namely a single exchange of two initially red electrons on the b -axis bond when both the other electrons on the cluster are green (this situation is represented in Fig. 7). There is thus no need to consider correlated hopping processes occurring on both c -axis bonds simultaneously (which are in fact available only for the $T_z = 0$ states of all four bonds on the plaquette), as these are of order t_e^4/U^3 . Thus at second order the plaquette-flipping matrix has the maximally sparse and inhomogeneous form

$$\begin{aligned} t_{+-,+} &= \frac{1}{2}J, \\ t_{\mu\nu,\rho\sigma} &= 0 \text{ otherwise.} \end{aligned} \quad (27)$$

This rather extreme form is due not only to the strict constraints set by the available color combinations, but also to the strong breaking of translational symmetry encoded in the choice of rhombic plaquette.

Under these circumstances, it is necessary to consider the second-order contributions to the QDM v term not contained in the dimer energy itself. From fluctuation processes on the three interdimer bonds one obtains

$$\begin{aligned} v_{+,+,+} &= -\frac{3}{4}J, \\ v_{+0,+} &= -\frac{3}{4}J, \\ v_{0+,0} &= -\frac{5}{8}J, \\ v_{+,-,+} &= -J, \\ v_{00,0} &= -\frac{3}{4}J, \\ v_{-+,-} &= -\frac{1}{2}J, \\ v_{0-,0} &= -\frac{3}{4}J, \\ v_{-0,-} &= -\frac{5}{8}J, \\ v_{---} &= -\frac{3}{4}J, \\ v_{\mu\nu,\rho\sigma} &= 0 \text{ otherwise.} \end{aligned} \quad (28)$$

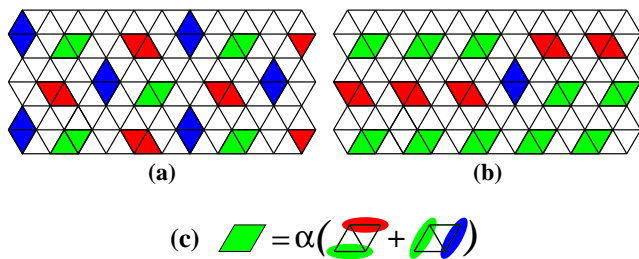


FIG. 8: (color online) Two plaquette coverings in the “columnar dimer” class which maximize the number of flippable plaquettes for (ss/ot) dimers on the triangular lattice. Shown are (a) a highly regular configuration with active plaquettes of all three orientations and (b) a more generic configuration of active plaquettes with two orientations plus a single “defect” of the third orientation. The color scheme represents the fact (c) that the ground state of each active plaquette is the symmetrized combination of states involving dimers with only two out of the possible three colors in the relevant orbital triplet; however, this triplet changes with the orientation of both the plaquette and the occupied bond.

The color constraint on the hopping possibilities is therefore sufficiently strong that the result is a diagonal v matrix. The non-uniformity in the diagonal values is due to the effect of the single b bond, from which one color configuration can profit maximally and one cannot profit at all, while the other combinations may use this to differing degrees.

From the manifestly strong effects on the t and v matrices arising from the choice of four-site plaquette units, one might conclude that symmetry-restoration effects due to summing over all of the available plaquettes and orientations are of prime importance, and that in this sense the consideration of a QDM does not advance the general understanding beyond that obtained in Ref. [1]. In the multicolored QDM, this strong breaking of symmetry will result in a selection process favoring only those dimer colors maximizing the contributions from quantum fluctuations, and hence in a system of $+$ and $-$ dimers on each active plaquette.

Whether it is possible to select the preferred dimer colors depends on the definition of the system. As in Sec. III, for models with no dimer number-mixing terms and fixed numbers of dimer of each color, the color sectors cannot mix and the system is constrained to maximize its energy with the available number of colors of each dimer. While the (os/st) case, in which the dimer color corresponds to the physical spin, is indeed constrained by this type of criterion (below), in the (ss/ot) case it is more straightforward to mix bond orbital sectors, as this can be done without changing the net electron orbital color balance, and therefore a selection of unequal numbers of T_z states is not restricted. Thus the effective QDM for the (ss/ot) case is a type of sector-switching two-color model with four matrix elements in v_{ij} and one in t_{ij} .

Such a model, with $|v| > |t|$ and, crucially, $v < 0$, is known to be in the “columnar” VBC state, the general

term applied to the set of dimer coverings which maximize the number of flippable plaquettes. Because of the constraint that $-+$ plaquettes are inactive for b -bond processes, the maximal number of active plaquettes obtainable in this “two-color” model is not the conventional $1/6$ but only $1/12$. The v and t terms select automatically the optimal color state of the spin singlets, and the ground state of each active plaquette is the symmetrized combination of “horizontal” and “vertical” dimer pairs with energy $-2J - |v| - t$. On the triangular lattice of N sites, the total number of valid plaquette states of this type is a highly (but not extensively – the entropy is proportional to the perimeter of the system) degenerate set, of which two examples are shown in Fig. 8. That the ground states are VBCs which break translational symmetry does not mean that the system has no positional fluctuations: rather, this type of configuration maximizes the sole kinetic (t) term present, but this is not strong enough to melt the static (v -driven) plaquette order. In this case, the QDM result is quite unambiguous: the ratio deduced for $|t/v|$ is well in the columnar phase, and not close to a boundary.

B. Superexchange limit, physical η

Here the ground state of the system is composed of (os/st) spin triplets. From the available electronic hopping processes, represented schematically in Fig. 9, it is clear that there is no second-order t term which can flip the orientation of a pair of (os/st) dimers. In contrast to the (ss/ot) case, the calculation of matrix elements thus requires the consideration of coherent electronic processes occurring at fourth order in the electronic Hamiltonian. For a meaningful comparison between fourth-order t and v terms in the relevant QDM, second-order contributions to v of the type computed in the previous subsection are treated as a renormalization of \tilde{J} . Let \tilde{J} denote $4t^4/(U - 3J_H)^3$, then

$$\begin{aligned} v_{\mu\nu,\mu\nu} &= -\tilde{J}, \\ v_{\mu\nu,\rho\sigma} &= 0 \text{ otherwise.} \end{aligned} \quad (29)$$

The spin-conservation symmetry (the absence of a magnetic field is assumed) makes the v matrix not only uniform but, in combination with the spin-pairing possibilities and the fact that electron hopping involves an automatic orbital color change, completely diagonal. The t matrix has more variety, because some overlap is per-

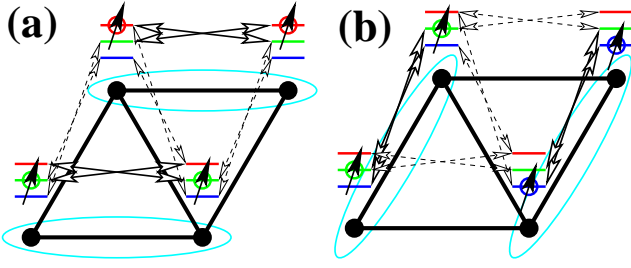


FIG. 9: (color online) Superexchange limit, (ac) plaquette, showing selected (a) horizontal and (b) “vertical” (os/st) dimer pairs (turquoise ellipses), along with a schematic representation of allowed electron hopping processes. Pairs of $S_z = 1$ triplets are depicted in both panels.

mitted within the sectors of fixed total spin, and thus

$$\begin{aligned}
 t_{+,+,+} &= t_{-,-,-} = \frac{1}{2}\tilde{J}, \\
 t_{+,0,+} &= t_{0+,0+} = \frac{1}{4}\tilde{J}, \\
 t_{00,00} &= \frac{1}{4}\tilde{J}, \\
 t_{0-,0-} &= t_{-,0,-} = \frac{1}{4}\tilde{J}, \\
 t_{+,0,+} &= t_{0+,+0} = \frac{1}{4}\tilde{J}, \\
 t_{+,-,00} &= t_{00,+} = \frac{1}{4}\tilde{J}, \\
 t_{-,0,00} &= t_{00,-} = \frac{1}{4}\tilde{J}, \\
 t_{-,0,-} &= t_{0-,-0} = \frac{1}{4}\tilde{J}, \\
 t_{\mu\nu,\rho\sigma} &= 0 \text{ otherwise.}
 \end{aligned} \tag{30}$$

In this case, there is blocking of the possible electronic processes leading to dimer flips by the allowed spin states: only the all-up and all-down spin configurations can profit from every available process. That the element $t_{00,00}$ is not symmetrical with $t_{+,+,+}$ and $t_{-,-,-}$ is a consequence of the breaking of translational symmetry in the plaquette choice.

In this case the system is not free to choose its color state, which would mean choosing its real magnetic state (in effect this defines another set of unmixable “topological” sectors characterized by the total S_z of the dimer ensemble). Under the reasonable assumption that the ground state will be net nonmagnetic, the system will have equal numbers of + and - triplets, but the ratio $N_{\pm} : N_0$ may lie anywhere between 0:1 and 1:0. The fact that matrix elements exist for many plaquette processes which mix the positions of 0 and +/- triplets suggests that it is most favorable for the system to preserve the option of fluctuating among all the possible states. If the system were to freeze, locally or globally, to either limiting case, the possibilities for dynamical fluctuations would be strongly reduced.

Thus one has deduced a true, three-color QDM, albeit one with predominantly diagonal elements in the 9×9 t and v matrices and with a ratio $t_{\mu\mu,\mu\mu}/v_{\mu\mu,\mu\mu} = -\frac{1}{4}$ for most components. This is again a system which is in a robust columnar phase. A columnar phase in a system with three dimer colors, all (for the sake of illustration)

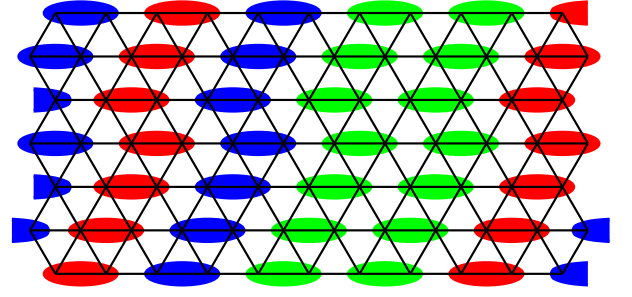


FIG. 10: (color online) A columnar dimer covering maximizing the number of flippable plaquettes on the triangular lattice for (os/st) dimers.

equally occupied, would be one with a one-dimensional nature (hard but flexible strings of dimers) of the type shown in Fig. 10.

Both in this case and for (ss/ot) dimers, individual matrix elements of v are rather larger than those in t . This result reflects the property of the model that all fluctuations away from and back to the starting configuration may contribute to v , while only quite specific pairs of color-switching processes are able to contribute to a t term. This places the system in the regime $|v| > |t|$ which is generically unsuitable for resonant states, and hence is the dominant physics deciding the (static or dynamic) nature of the ground state; the type of static phase is in turn determined by the sign of v . While it is again necessary to consider the restoration of translational symmetries broken rather crudely at the four-site plaquette level, it is difficult to conceive of circumstances under which this would bridge the gap, which includes changing the sign of v , from the columnar phase to an RVB phase.

To conclude the analysis of this and the previous subsection, from effective QDMs it appears very likely that the t_{2g} superexchange models on the triangular lattice favor “columnar” VBC states. In the (ss/ot) case this is a type of two-color model with plaquette-ordered ground states, while in the (os/st) case it is a three-color model with dimer-ordered ground states. These states break the symmetry both in real space (lattice translation and rotation) and in the space of dimer color. This result is a consequence of the fact that virtual fluctuations promoting dimer resonance are simply too restrictive (in “color”, be this the orbital type or the real spin) to be numerous enough to compete qualitatively with virtual fluctuations profiting from static order.

C. Direct-exchange limit, $\eta = 0$

As demonstrated in Sec. II, in this model (17) the dimer overlap factor is $\alpha = 0$. Thus the model is naturally color-conserving. The conventional QDM plaquette terms are simply $t = 0 = v$ and the appropriate model is obtained from 6-bond, 3-dimer loops of the type shown in Fig. 3 (for which there are two orientations). These

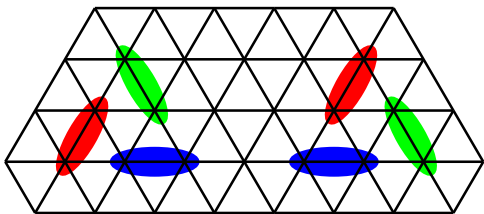


FIG. 11: (color online) Representation of the six-bond triangular loop fluctuation which is the minimal kinetic process permitted in the direct-exchange limit.

contribute at sixth order in the electronic Hamiltonian, both to a v' term for processes returning to the starting configuration and to a t' term for correlated hopping processes in the same direction around the triangle, which lead to a net shift of the dimer positions. For clarity this is illustrated again in Fig. 11, with the dimers retaining their color code (which here, in contrast to the preceding subsections, does denote their orbital state). By analogy to the procedure mentioned above, fourth-order contributions to maintaining the static dimer configuration can also be renormalized into the energy of the dimer coverings (whose extensive degeneracy is not affected by these). By writing out the wave functions for the triangle states,

$$|\psi_t^l\rangle = \frac{1}{2\sqrt{2}}(|1b\uparrow 2b\downarrow\rangle - |1b\downarrow 2b\uparrow\rangle)(|3g\uparrow 4g\downarrow\rangle - |3g\downarrow 4g\uparrow\rangle)(|5r\uparrow 6r\downarrow\rangle - |5r\downarrow 6r\uparrow\rangle), \quad (31)$$

$$|\psi_t^r\rangle = \frac{1}{2\sqrt{2}}(|2b\uparrow 3b\downarrow\rangle - |2b\downarrow 3b\uparrow\rangle)(|4g\uparrow 5g\downarrow\rangle - |4g\downarrow 5g\uparrow\rangle)(|6r\uparrow 1r\downarrow\rangle - |6r\downarrow 1r\uparrow\rangle), \quad (32)$$

and proceeding in a manner analogous to the previous two subsections, one finds

$$v' = -576 \frac{t_e^6}{U^5}, \quad t' = \frac{603}{2} \frac{t_e^6}{U^5}. \quad (33)$$

As above, the difference in magnitude between v' and t' arises due to the prevalence of connected processes not changing the dimer configuration over those leading to the specific resonance loop in question.

Thus once again this is a model strongly in the columnar limit: based on a predominant ordering pattern and profiting from limited fluctuations (occurring only on selected generalized plaquette units). The meaning of the term “columnar” in standard QDM literature is a configuration maximizing the number of flippable plaquettes, which for the $t'-v'$ model means the number of up- and down-oriented triangles. Examples are shown in Fig. 12. This columnar ground state has three possible color combinations, specifically those where any two colors are used in two triangles each, plus a triangle chirality, and hence is six-fold degenerate. It does not possess equal numbers of dimers of each color (the ratio is 1:1:2). A ground state of a macroscopic system may be expected to have a domain structure, and all states with equal dimer numbers will present defective versions of this phase.

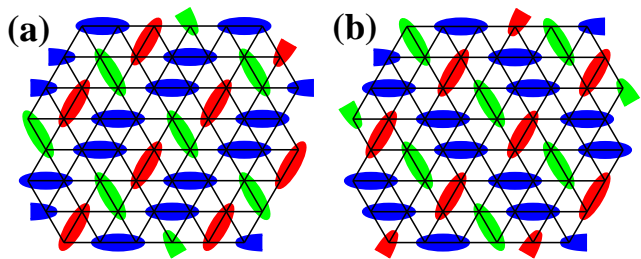


FIG. 12: (color online) “Columnar” dimer coverings of the triangular lattice maximizing the number of flippable six-site triangular units. Two of the six possibilities are illustrated: in panel (a) the red and green dimers (directions) each participate in two loops and the more numerous blue dimers in one; in panel (b) is shown the inequivalent state which still has blue as the unique direction but has the opposite chirality of dimer locations on the the up- and down-oriented triangular units.

The overall energy gain of this state of the QDM relative to the original manifold (which has $e_{\text{VB}} = -J'/6$) is $e = (v - t)\langle n_{\text{fl}} \rangle$ per plaquette, which in the present case of six-bond loops is $e_6 = (v' - t')/12 \simeq -73t_e^6/U^5$ per bond. However, because of the higher-order nature of this correction, it is not able to alter the conclusion¹ that the one-dimensional solution, which has energy $e_{1\text{D}} = -\frac{1}{3}\ln 2 = -0.23105J'$ per bond, appears to lie lower than all dimer states. It is worth reiterating in this context that the present considerations are restricted to the case when η is identically zero; as noted in Sec. II, finite values of η lead to the stabilization of particular static VBC configurations which promote energy gains of $O(\eta^3)$,⁹ also insufficient to redress the energy balance. The prevalence of the one-dimensional solution in a geometry of such high connectivity is testimony to the enormous degree of orbital-induced frustration in the full physical system.

V. SUMMARY

This manuscript pursues, by mapping to a set of quantum dimer models (QDMs), the nature of the ground state of the t_{2g} spin-orbital model on the triangular lattice. The electronic Hamiltonian, investigated in detail in Ref. [1], represents an insulating $3d^1$ electron system on the $\langle 111 \rangle$ planes of a system such as NaTiO_2 , where the cubic structural symmetry of edge-sharing metal-oxygen octahedra leads to an unbroken, threefold orbital degeneracy. This model was shown¹ to have a very strong preference for dimer-based states of no long-ranged magnetic or orbital order over its entire parameter range in both the ratios J'/J (of the direct and superexchange contributions to the magnetic interactions) and J_H/U (of the Hund coupling to the on-site Coulomb repulsion).

These dimer states were found to span a range of behavior from highly resonant in the superexchange limit to quasi-static in the direct-exchange limit. Both cases

present fundamental challenges in determining the nature of the true ground state: the former is a candidate resonating valence-bond (RVB) state and the latter a situation where subtle selection effects, sometimes known as “order-by-disorder,” are responsible for choosing the true ground state from a very highly degenerate manifold. In Ref. [1] only energetic studies were performed, which were unable to answer the topological questions associated with the formation of an RVB state or to resolve the possible differences among quasi-static valence-bond coverings.

These questions are addressed by mapping the electronic Hamiltonian to the minimal QDM for each of three cases: (a) the pure superexchange limit for low J_H/U , (b) the pure superexchange limit for intermediate J_H/U , and (c) the direct-exchange limit for $J_H/U = 0$. In case (a), the ground state is composed of spin-singlet, orbital-triplet (ss/ot) dimer entities and the effective QDM has three dimer “colors” corresponding to their orbital state. In case (b), the ground state is composed of orbital-singlet, spin-triplet (os/st) dimers and the effective QDM has again three colors, which correspond to the triplet spin components of the dimers. In case (c), there are three dimer colors corresponding to the orbital colors active in each of the three bond directions of the triangular lattice, but because these are locked to each other, the color is not a degree of freedom and the effective QDM has one color. The “non-orthogonality catastrophe” which affects conventional spin dimers, namely that all dimer coverings have finite overlap, is shown to be very strongly reduced or completely eliminated in the presence of a dimer color in such models.

In order to analyze the properties of these specific QDMs, first the general multicolored QDM must be understood. This is investigated for the two-color case, with some additional consideration of three-color QDMs where these contain further physics. Both the potential term v for adjacent dimers and the kinetic term t for these to flip direction on the four-site plaquette they define become $n^2 \times n^2$ matrices, where n is the number of colors. With such a choice of matrix elements, there remains only one Rokhsar-Kivelson (RK) point, where the equally weighted superposition of all possible dimer coverings (in a given topological sector) is an eigenstate, but the regime of parameters in which this (gapped, RVB) state is the ground state is expanded considerably. Non-trivial topological sectors are found for specific choices of matrix elements, notably those conserving the total number of dimers of each color and those which allow this to be altered not in single steps but in units of two. This gives rise to topological excitations related to the color degree of freedom, which are termed “color visons.”

The matrix elements $t_{\mu\nu,\rho\sigma}$ and $v_{\mu\nu,\rho\sigma}$ are deduced from the electronic Hamiltonian for cases (a) and (b). The restrictions on hopping of electrons of different orbital color and the breaking of translational symmetry contained in the consideration of four-site plaquettes lead

in case (a) to very sparse and asymmetric matrices. This asymmetry selects only the $T_z = \pm 1$ orbital triplet states, and the model is reduced to one with two colors. In case (b), the physical spin defines “topological” sectors which cannot mix. In both cases, elements of the v matrix are generally rather larger than those of the t matrix, and have in addition a negative sign. Thus the mapping to a QDM indicates strongly that the ground state of both models is a “columnar” plaquette phase, one which is based on a small subset of static dimer coverings which maximize the number of flippable four-site plaquettes: this number is 1/12 of the total in case (a) and 1/6 in case (b). While these states gain energy from virtual dimer flipping processes (quantum fluctuations), such processes are not sufficiently strong that they can “melt” the plaquette or dimer order in favor of a completely resonant, symmetry-restored phase.

In case (c), the overlap matrix elements, and t and v elements, on a four-site plaquette are identically zero. The leading quantum fluctuation processes for dimer resonance occur on six-site, triangular units containing one dimer of each bond direction, and hence the corresponding minimal QDM is a $t'-v'$ model defined on these “plaquettes”. Once again, v' is negative and larger in magnitude than t' , suggesting that the ground state of the system is again a generalized columnar covering (meaning one which maximizes the number of flippable triangles). These are illustrated and shown to have a six-fold degeneracy, corresponding to the bond direction and the triangle chirality.

In summary, effective QDMs are used to obtain indications as to the nature of the ground state of a complex electronic Hamiltonian for a spin-orbital model which is known to have no conventional magnetic or orbital order. In all cases of most interest, the ground state is found to be a resonance-stabilized spin-orbital VBC covering which maximizes quantum fluctuation processes on a restricted set of plaquettes, but does not allow the melting of a preferred order by these fluctuations. While the derivation of a QDM involves rather crude symmetry-breaking at the level of four- (or six-)site plaquettes, and the symmetry-restoring effects of fluctuations across all available plaquettes must be borne in mind, the columnar phases deduced from all three QDMs are quite robust, indicating that there is no nearby liquid phase.

Acknowledgments

The author is especially grateful for the invaluable contributions of G. Jackeli. Thanks are due also to D. Ivanov and F. Mila for helpful discussions. This work was supported by the National Science Foundation of China under Grant No. 10874244 and by Chinese National Basic Research Project No. 2007CB925001.

-
- ¹ B. Normand and A. M. Oleś, Phys. Rev. B **78**, 094427 (2008).
- ² see R. Moessner and K. S. Raman, in *Highly Frustrated Magnetism*, eds. C. Lacroix, P. Mendels, and F. Mila (Springer, Heidelberg, 2010), and references therein.
- ³ F. Mila, F. Vernay, A. Ralko, F. Becca, P. Fazekas, and K. Penc, J. Phys.: Condens. Matter **19**, 145201 (2007).
- ⁴ D. S. Rokhsar and S. A. Kivelson, Phys. Rev. Lett **61**, 2376 (1988).
- ⁵ R. Moessner and S. L. Sondhi, Phys. Rev. Lett **86**, 1881 (2001).
- ⁶ F. Vernay, A. Ralko, F. Becca, and F. Mila, Phys. Rev. B **74**, 054402 (2006).
- ⁷ G. Chen, L. Balents, and A. P. Schnyder, Phys. Rev. Lett. **102**, 096406 (2009); G. Chen, A. P. Schnyder, and L. Balents, Phys. Rev. B **80**, 224409 (2009).
- ⁸ K. I. Kugel and D. I. Khomskii, Usp. Fiz. Nauk **136**, 621 (1982) [Sov. Phys. Usp. **25**, 231 (1982)].
- ⁹ G. Jackeli and D. A. Ivanov, Phys. Rev. B **76**, 132407 (2007).
- ¹⁰ X.-G. Wen, *Quantum Field Theory of Many-Body Systems*, (OUP, Oxford, 2004).
- ¹¹ A. Ralko, M. Ferrero, F. Becca, D. Ivanov, and F. Mila, Phys. Rev. B **71**, 224109 (2005).
- ¹² A. Ioselevich, D. A. Ivanov, and M. V. Feigelman, Phys. Rev. B **66**, 174405 (2002).
- ¹³ P. W. Kasteleyn, J. Math Phys. **4**, 287 (1963); S. Samuel, J. Math Phys. **21**, 2806 (1980).